

Varying Magnetization Orientation for Permanent-Magnet Volume Reduction in Machines

Maxime R. Dubois, *Member, IEEE*, Henk Polinder, *Member, IEEE*, and Jan Abraham Ferreira, *Senior Member, IEEE*

Abstract—We present an enhanced version of a method to minimize the amount of permanent-magnet (PM) material required to create a certain flux linkage in the stator winding of a PM machine. The enhanced version obtains the distribution of the factor δ inside the PM; δ identifies the areas inside the PM volume where the orientation of magnetization may be modified, so as to further increase the amount of no-load flux linkage generated by the PM per cubic meter of PM material. The paper shows how this method can be used with increased benefits in machines with small pole pitches. The case of a transverse-flux permanent-magnet (TFPM) machine with a pole pitch of 1 cm is analyzed. The resulting PM design shows an improvement of 48% of the amount of flux linkage created per volume of PM material, for the same air-gap thickness and magnet thickness.

Index Terms—Cost optimization of machines, direction of magnetization, permanent-magnet shaping, transverse-flux permanent-magnet machines.

I. INTRODUCTION

THE availability of permanent magnets (PM) with high remanent flux densities, such as Nd-Fe-B and Sm-Co magnets, offers interesting possibilities to electrical machines designers. Among other advantages, it becomes possible to create cheaper machines. As discussed in [1], conventional PM synchronous machines may have pole pitches shorter than conventional wound-rotor synchronous machines. In many cases, small pole pitches will lead to a reduction in the amount of copper for the stator end windings, as well as a reduction in the amount of steel for the stator yoke and rotor back iron. Even though PMs help in reducing the total volume of copper and steel, most PM materials are expensive. Nowadays, sintered Nd-Fe-B magnets can be purchased for about 35 US\$/kg, while the cost of standard 0.5-mm-thick steel laminations is around 1.5 US\$/kg. In many cases, the cost of PM material is a significant part of the total machine cost.

One way of decreasing the cost of those machines is to reduce the volume of PMs. This paper addresses the minimization of PM volume by increasing the no-load flux linkage λ_{PM} created in the stator coils per cubic meter of PM material. The first step in the design of PMs in machines is the determination of magnet

thickness using the assumption of rectilinear fields in the air gap. As a second step, the magnet shape can be arranged, to take into account the leakage between magnets and other effects due to the two- and three-dimensional (2-D and 3-D) distribution of the fields.

A method was developed in [2] for the shaping of PM material. This maximization method is used with PM material having relative recoil permeabilities close to unity and ideal steel. It determines whether each volume element dv inside the PM has a high or a low contribution to the no-load flux linkage. The PM is shaped so as to remove the elements with the lowest contribution. The result is a higher ratio of no-load flux linkage λ_{PM} per volume V_{PM} of PM material.

In the first part of the paper, the optimization method described in more detail in [2] will be summarized. In the second part of the paper, the orientation of magnetization of the remanent flux density B_r is varied inside the PM volume. A factor δ is introduced, which is distributed throughout the volume of the PM. For values of δ different from unity, the orientation of B_r inside the PM may be modified, increasing the amount of flux linkage created.

The method is especially beneficial for PM machines with short pole pitches. Such machines have a large part of their fields traveling in 2-D. In the paper, the method is applied to the magnet shaping in a transverse-flux machine with single-sided surface-mounted (SSSM) PM. This type of machine is described in detail in [3]. In most cases found in literature [3]–[5], transverse-flux permanent-magnet (TFPM) machines have small pole pitches (in the order of 1 cm). It will be shown that applying this method to the TFPM SSSM configuration significantly increases the flux linkage generated by the rotor in the stator winding, per cubic meter of PM material.

II. FIRST STEP: DETERMINATION OF PM VOLUME AS PART OF THE TOTAL MACHINE OPTIMIZATION

Determination of the magnet volume is usually done as part of a total machine optimization, as done in [1]. For example, the parameter to be optimized may be cost, mass, or machine volume, while efficiency, losses, or inertia may be one of the constraints imposed to the optimization process. In itself, magnet volume will seldom be the objective of the optimization function within this first step of the optimization process. Often, the PM thickness is established, considering all fields in the air gap as rectilinear (i.e., 1-D), in order to simplify the optimization.

Manuscript received June 22, 2001; revised February 3, 2003. This work was supported in part by Delft University of Technology and in part by the FCAR, Quebec, Canada.

The authors are with the Delft University of Technology, 2628 CD Delft, The Netherlands (e-mail: m.dubois@its.tudelft.nl; h.polinder@its.tudelft.nl; j.a.ferreira@its.tudelft.nl).

Digital Object Identifier 10.1109/TMAG.2003.809864

Once the magnet thickness has been set up using the assumption of rectilinear fields and rectangular PMs, the criterion of high λ_{PM}/V_{PM} may be used to optimize PM volume in the presence of 2-D and 3-D fields. This is the subject discussed in the remainder of this paper.

III. SECOND STEP: METHOD OF PM SHAPING FOR HIGHER FLUX LINKAGE PER PM VOLUME FOR 2-D AND 3-D FIELDS

A. Mathematical Expression for the No-Load Flux Linkage as a Function of the PM Geometry

The conventional expression used to calculate the no-load flux linkage λ_{PM} is given by

$$\lambda_{PM} = \int_{S_{coil}} \int \vec{B}_{PM} \cdot d\vec{s}_{coil} \quad (1)$$

where λ_{PM} is the flux linkage obtained in the stator coil at no-load, \vec{B}_{PM} is the magnetic flux density created by the PM everywhere in space, and S_{coil} is the area bounded by the stator coil. The surface element $d\vec{s}_{coil}$ is a vector, which direction is normal to the coil surface at a given location and which length is proportional to the surface element. Equation (1) expresses the no-load flux linkage as a vector quantity created by the PM (\vec{B}_{PM}), acting on the coil geometry (S_{coil}).

In [2], a mathematical expression is derived, giving λ_{PM} in a reciprocal manner, that is as a vector quantity created by the coil (magnetic field \vec{H}_a) and acting on the PM geometry, as given by

$$\lambda_{PM} = \int_{V_{PM}} \int \int \left[\frac{\vec{H}_a}{i} \right] \cdot \vec{B}_r dv \quad (2)$$

where \vec{H}_a is the magnetic field intensity created by the coil alone, when a current i flows in that coil. As described in [2], the magnetic field \vec{H}_a is computed when all PMs are replaced by vacuum. \vec{B}_r is the remanent flux density inside the volume V_{PM} of the PM.

The expression of λ_{PM} given by (2) is mathematically equal to (1) only if the following assumptions are used.

- PM material has linear $B(H)$ characteristic and unity recoil relative permeability. The $B(H)$ curve inside the PM volume is assumed to be given by (3)

$$\vec{B} = \mu_0 \vec{H} + \vec{B}_r. \quad (3)$$

- The steel inside the machine has infinite permeability and does not saturate.
- The variation of the magnetic vector potential \vec{A}_{PM} inside the conductors is negligible compared to the value of \vec{A}_{PM} at the border of the conductors.

In many cases, PM machines satisfy these assumptions. Rare-earth PM materials, such as Nd-Fe-B and Sm-Co, have recoil relative permeabilities in the vicinity of 1.1. As discussed further in the paper, these assumptions can be used without significant consequences on the final conclusions.

Equation (2) describes the no-load flux linkage λ_{PM} as a mathematical function integrated over the PM volume. For every volume element dv inside the volume of the PM, each of

these volume elements dv can be given a certain contribution to the total flux linkage. It becomes possible to trace volume elements with a higher contribution and those with a lower contribution.

B. Method for the Shaping of PM

Using (2), a method has been developed in [2] to eliminate the parts inside the PM volume, which have a low contribution to the no-load flux linkage in the stator winding. This maximization method is applied as a second step in the design of PM shapes. If \vec{H}_a is a 2-D or 3-D function of space and therefore has variable magnitude and orientation in the air gap, the application of this method results in an increasing ratio of no-load flux linkage λ_{PM} over PM volume V_{PM} . The method may use either finite-element analysis (FEA) or analytical calculation in the following manner.

- Consider the rotor position for which PMs are aligned with the stator poles. This is the position of maximum flux linkage under no-load conditions.
- Replace all PM by vacuum (in the FEA model, or in the analytical model).
- Inject a current i in the coil for which we want to calculate the no-load flux linkage.
- All other coils have $i = 0$.
- Calculate the field \vec{H}_a inside the volume that would normally contain PM material.
- Compute the dot product of \vec{H}_a with \vec{B}_r . This will give out the contribution of each volume element inside the PM.
- Remove the volume elements with the lowest contribution.

IV. PM SHAPING IN TFPM SSSM MACHINES

The proposed method can be used to obtain optimized shapes of PM for virtually any kind of PM machines. As pointed out in [2], the ratio of no-load flux linkage λ_{PM} over PM volume V_{PM} cannot be significantly increased if most of the stator-created magnetic field \vec{H}_a travels in one dimension inside the volume of the rotor magnets.

In machines where the pole pitch is short and where a large part of the stator-created magnetic field \vec{H}_a travels in two or three dimensions inside the rotor magnets, the proposed shaping method may reduce significantly the amount of PM material required to create a given no-load flux linkage. Transverse-flux machines are usually used with small pole pitches, where the amount of fringing field \vec{H}_a is important. As will be shown in this section, interesting benefits can be expected with the use of the proposed method on TFPM SSSM machines. The TFPM SSSM is shortly described here.

A. Description of the TFPM SSSM Machine

The TFPM SSSM machine [3] is shown in Fig. 1. The main characteristic of TFPM machines is the independence between the amount of stator-created MMF and the rotor-created no-load flux linkage.

In other words, the window in which the conductors are placed can be made many times wider than the pole pitch, which is not the case with conventional PM longitudinal machines. This allows the pole pitch in the TFPM SSSM of

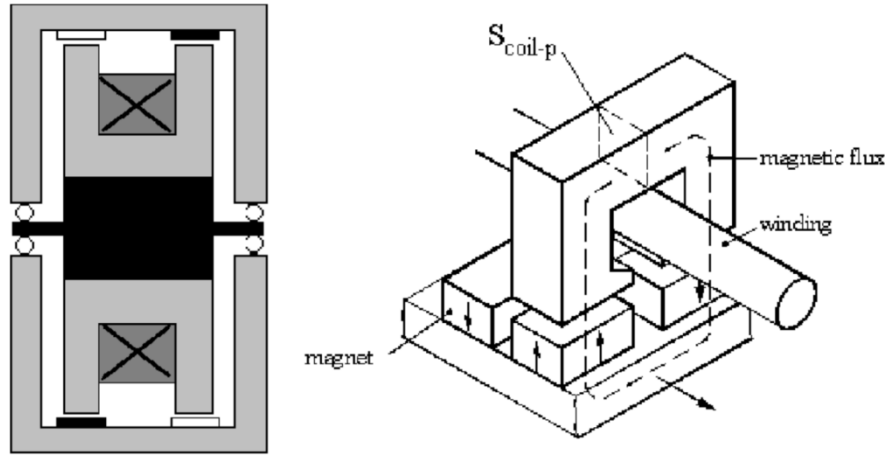


Fig. 1. Cross-sectional and 3-D views of a TFPM SSSM machine.

Fig. 1 to be made very small, while still keeping a large winding window area. Small pole pitches increase the rate of change of the no-load flux linkage, which in turn increase the no-load voltage.

The TFPM SSSM machine is composed of C-cores in the stator, mounted on the interior part of the machine. The stator winding is made of one single coil wound on top of the inner part of the C-cores. This conductor can be wound on itself to create a coil with several turns in series. The PMs are placed on the inner part of the outer ring and face the C-core heads. There are four PMs per C-core, which are placed with alternate polarities. For each C-core, two of these PMs face the stator C-core heads, while the two remaining PM exchange magnetic flux through air.

B. Local Contributions of PM Volume Elements in a TFPM SSSM Machine

For this study, we will use a pole pitch of 1 cm, which is also the value that was used in [3]. In this configuration, the pole pitch is defined as the total air-gap perimeter of the machine divided by twice the number of C-cores. All other dimensions are given in Appendix I, for the four different magnet shapes analyzed in the paper.

The first shape is shown in Fig. 2, where the magnets are rectangular, with no clearance between them. Each magnet has a uniform value of B_r inside its volume (uniform magnitude and orientation).

The method proposed in Section III-B is applied to the configuration of Fig. 2. The PMs are replaced by vacuum and a current $i = 10$ A is injected in the one coil of the stator winding. With the use of a 2-D FEA software, the distribution of the magnetic field H_a is obtained inside the volume of the PMs. It must be noted that in the TFPM configuration, the current in the coil excites all the C-cores simultaneously. We may write the total flux linking the coil

$$\lambda_{PM} = p \int_{V_{PMp}} \int \int \left[\frac{\vec{H}_a}{i} \right] \cdot \vec{B}_r dv \quad (4)$$

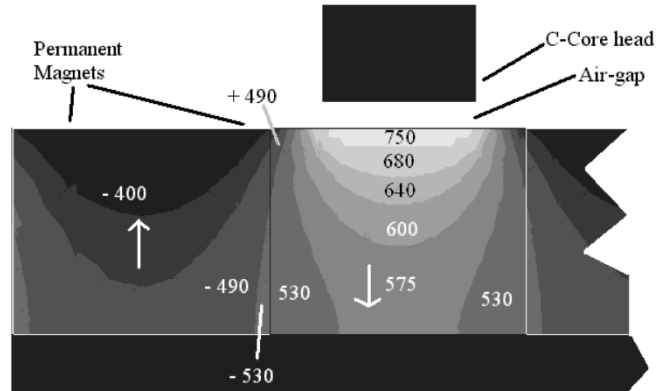


Fig. 2. Dot product of H_a and B_r inside the volume of the PM of a TFPM SSSM machine. PMs are adjacent block Nd-Fe-B magnets. MMF injected in the stator is $ni = 10$ A-turns. The other C-core heads are not shown, but are also excited by the current i .

where p is the number of C-cores (or pole pairs) in the machine and V_{PMp} is the total volume of PM per C-core. The no-load flux linkage is computed by integrating $H_a \cdot B_r$ over the cross section of the magnet. Because a 2-D analysis is used, the integral is computed on a cross section, instead of a volume. The surface integral gives a no-load flux linkage per pole pair of 0.00198 Wb/m.

The no-load flux linkage obtained with (4) is compared to the conventional method of computing the no-load flux linkage, given by

$$\lambda_{PM} = np \int_{S_{coil-p}} \int \vec{B}_{PM} \cdot d\vec{s}_{coil} \quad (5)$$

where S_{coil-p} is the surface of one C-core yoke linking the coil and n is the number of turns in the stator coil. The no-load flux linkage per C-core is calculated using both expressions, and the results are given in Table I. The two methods give comparable results and the difference observed between the results obtained with (4) and (5) is 8%. This difference is explained by the use of PM material in the FEA model, which have a recoil relative permeability of $\mu_{rec} = 1.09$, where (4) assumes $\mu_{rec} = 1$. As shown in Table I, the total cross section of PM per C-core is

TABLE I
FEA RESULTS FOR FOUR DIFFERENT PM CONFIGURATIONS

PM Shape	λ_{PM} given by $\iint_{S_{out}} \vec{B}_{out} \cdot d\vec{S}_{out}$	λ_{PM} given by $\iiint_V \left[\frac{\partial H_a}{\partial i} \right] \cdot \vec{B}_r \cdot dv$	Error $\Delta \lambda_{PM}$	PM cross-section per pole pair	λ_{PM}/V_{PM}
	(Wb/m)	(Wb/m)	(%)	(mm ²)	(Wb/m ³)
Square PM 100% (fig. 2)	0.00215 ($\mu_{rec}=1.09$)	0.00198 ($\mu_{rec}=1.00$)	8	320	6.7 ($\mu_{rec}=1.09$)
Square PM 80% (fig. 3)	0.00205 ($\mu_{rec}=1.09$)	0.00190 ($\mu_{rec}=1.00$)	7	256	8.0 ($\mu_{rec}=1.09$)
V-shape PM (fig. 4)	0.00188 ($\mu_{rec}=1.09$)	0.00173 ($\mu_{rec}=1.00$)	8	204	9.2 ($\mu_{rec}=1.09$)
V-shape PM with varying B_r (fig. 7)	0.00207 ($\mu_{rec}=1.09$)	0.00195 ($\mu_{rec}=1.00$)	6	210	9.9 ($\mu_{rec}=1.09$)

320 mm². As a result, we have a flux linkage of 6.7 Wb/m³ of PM material.

To identify the contribution of each volume element dv inside the PM, the dot product of the resulting magnetic field H_a with the remanent flux density B_r inside the volume of the PM is calculated with an FEA software and shown in Fig. 2. This plot indicates the contribution of each volume element inside the PM to the no-load flux linkage created in the coil.

From Fig. 2, it appears that the two adjacent magnets cancel each other, because the magnet facing the C-core head has positive values of $H_a \cdot B_r$, while the magnet on the left-hand side has negative values. However, the cancellation is not complete because the positive values in the middle of the magnet facing the C-core head (up to 750 J/m³) are higher than the absolute value obtained in the middle of the magnet on the left-hand side (400 J/m³).

It is common practice to select magnet blocks having a span of 80% of the pole pitch. From Fig. 2, this practice seems reasonable, because the PM elements near the border have almost equal absolute values of $H_a \cdot B_r$, but with opposite signs. In other words, the contribution of the volume elements near the PM frontier almost cancel one another.

Removing 20% of the PM cross section, as shown in Fig. 3, and calculating the no-load flux linkage with the conventional (5) and new (4) expressions for flux linkage, we obtain a reduction of 5% in the no-load flux linkage, while the total PM cross section is reduced by 20%. The amount of flux linkage per PM volume has increased to 8.0 Wb/m³. These results are shown in Table I and the difference in no-load flux linkage obtained with the two mathematical expressions for λ_{PM} is 7%, which again is explained by a difference in the recoil permeabilities used.

Using the plot of Fig. 2, we select the areas inside the PM where the values of $H_a \cdot B_r$ are low. With the constraint of symmetrical magnets, we remove the areas in both magnets with low values of $H_a \cdot B_r$.

By inspection of Fig. 2, a better magnet shape may be obtained if the magnet has a V-shape, as shown in Fig. 4.

The total cross section of this new magnet shape is 204 mm² per C-core, and the integration of (4) over the PM cross section

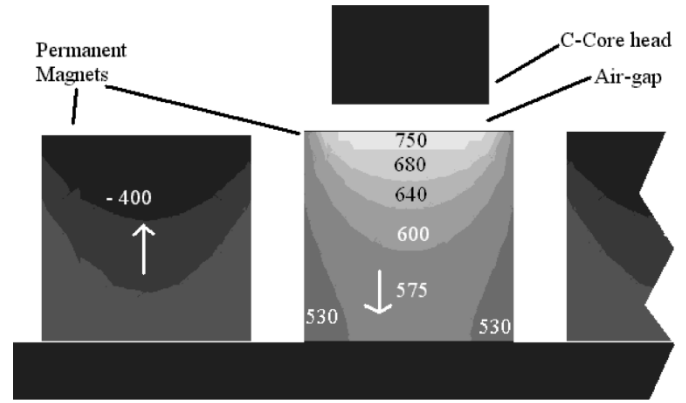


Fig. 3. Dot product of H_a and B_r inside the volume of the PM of a TFPM SSSM machine. PMs are rectangular Nd-Fe-B magnets. MMF injected in the stator is $i = 10$ A-turns. The magnets have a width of 8 mm, and the distance between two adjacent magnets is 2 mm.

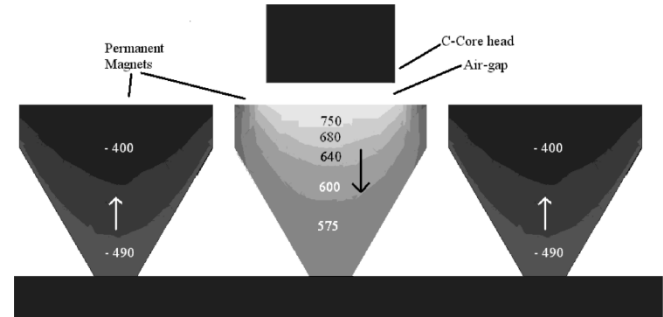


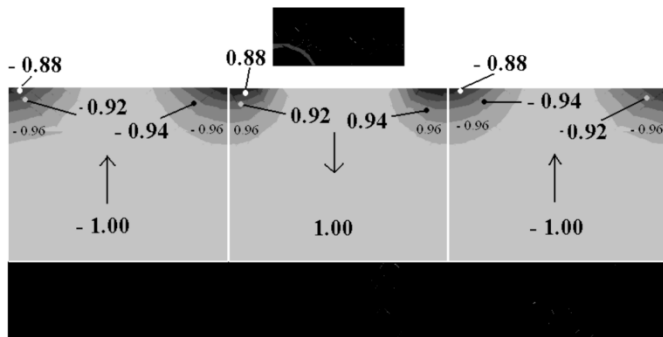
Fig. 4. Dot product of H_a and B_r inside the volume of the PM of a TFPM SSSM machine. PM are V-shaped Nd-Fe-B magnets. MMF injected in the stator is $i = 10$ A-turns. The top part of the magnet has a width of 9 mm, and the bottom part a width of 2 mm.

gives a flux linkage of 0.00188 Wb/m per pole pair. The amount of magnet material has decreased by 36.3% compared to the first magnet configuration of Fig. 2. The no-load flux linkage has decreased by 12.6%. The amount of flux linkage per volume of PM material has increased to 9.2 Wb/m³, an increase of 37% compared to the block magnets with a span of 100% (Fig. 2).

By inspection of Fig. 2, it must be noted that even higher ratios of flux linkage over PM volume can be obtained, without changing the field H_a , and while keeping the distance between the stator C-core head and the rotor iron as shown in Fig. 2. This can be realized if only a thin layer of PM material is kept in the top part of the PM, where the dot product of $H_a \cdot B_r$ is 750 J. Such a shape would give a high ratio of flux linkage over PM volume (up to 17 Wb/m³ is possible). Even though the cost of PM material will be reduced, the amount of flux and power will also be significantly lowered. If cost has to be minimized, one must keep in mind that PM material is only one of the components in a machine and that other components must also be taken into account. Also, such a very thin layer of PM will be subject to demagnetization, when a current i is fed to the coil.

V. VARIATION OF B_r ORIENTATION

In this section, the PM optimization method described in Section III-B is enhanced with an additional step. This new step uses


 Fig. 5. Distribution of δ inside the PM volume.

the theoretical result given by (4). The ratio of flux linkage over PM volume can be increased by varying the orientation of B_r inside the PM. Equation (4) describes the flux linking the stator coil at no-load as the integral of a dot product of H_a and B_r . In machines with large pole pitches, most of the field lines of H_a are aligned with B_r . However, in machines with small pole pitches, such as TFPM SSSM machines, a large part of the field lines of H_a are not aligned with B_r . As a consequence, the cosine of the angle between H_a and B_r gives a value below 1. This has an impact on dot product of H_a and B_r . The method of Section III-B is enhanced with the inclusion of a plot of δ , as given by

$$\delta = \frac{\vec{H}_a \cdot \vec{B}_r}{\|\vec{H}_a\| \|\vec{B}_r\|} \quad (6)$$

where δ is the cosine of the angle between H_a and B_r at any given point inside the PM. A plot of δ inside the volume of the PM is illustrated in Fig. 5, after injection of a current $i = 10$ A.

Fig. 5 indicates values for δ varying between 0.88 and 1 in the PM facing the C-core head and values varying between -0.88 and -1 for the magnet on the left-hand side. A value of $\delta = 0.9$ corresponds to an angle of 26° between H_a and B_r . With the information presented in Fig. 5, it is possible to select areas inside the PM where a rotation of B_r will increase the product of $H_a \cdot B_r$. The area where $\delta = 1$ is not of interest, because δ already has the highest value. However, the upper corners are subject to a potential increase, if the angle of B_r is modified. This will increase the value of $H_a \cdot B_r$ in those areas and the contribution of those PM volume elements to the total flux linkage will be increased.

Fig. 6(a) illustrates a zoom in the upper corners of two adjacent magnet blocks before modification. The vectors H_a and B_r are shown inside those two corners. The contribution of the right corner is almost cancelled by the negative contribution of the left corner. In Fig. 6(b), the orientation of B_r inside the two corners has been modified, so as to align H_a and B_r inside the corner of the PM facing the C-core. By symmetry, the orientation of B_r must also be modified in the corner of the PM not facing the C-core. As shown in Fig. 6(b), the angle between H_a and B_r has increased further on the left-hand side, reducing the negative contribution of the left corner. The change in B_r orientation brings a double improvement to the no-load flux linkage, by increasing the positive contribution and reducing the negative contribution.

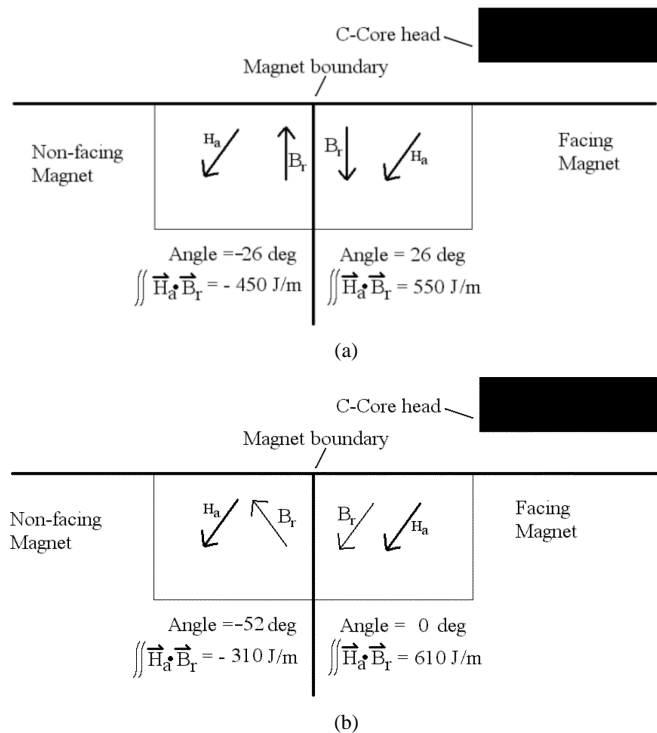


Fig. 6. (a) Orientation of B_r before modification. The product of $H_a \cdot B_r$ on the right corner is almost cancelled by the product of $H_a \cdot B_r$ on the left corner. The total sum of the two is 100 J/m. (b) Orientation of B_r after modification. B_r is aligned with H_a in the right corner. In the left corner, the angle between H_a and B_r is increased. The total sum of $H_a \cdot B_r$ in that area is now 300 J/m.

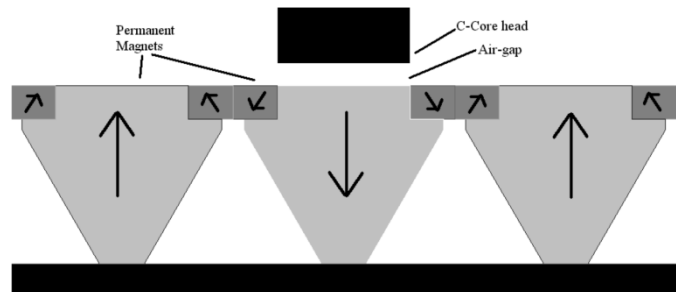


Fig. 7. New magnet arrangement proposed to increase the flux linkage per PM volume. Small magnets are inserted in the corners of the main magnets. The angle between the B_r of each small magnet and the B_r of the main magnet is 26° .

Fig. 7 illustrates the proposed magnet shape and new orientation of B_r inside the magnet. Each corner of the magnets now makes an angle of 26° with the main axis. The new configuration with small corner magnets creates a flux linkage of 0.00207 Wb/m per pole pair. The PM cross section per pole pair is 210 mm². The ratio of no-load flux linkage over PM volume has now increased to 9.9 Wb/m³. This is an increase of 8% compared to the V-shape of Fig. 4 and an increase of 48% compared to the initial block magnets of Fig. 2. In fact, the configuration of Fig. 7 has only 3.7% less flux linkage, for 34% less PM material than the first PM configuration of Fig. 2.

The final distribution of the dot product of H_a and B_r with modified V-shape and corner magnets with a 26° angle is shown in Fig. 8. Comparing with the distribution of Fig. 2, it is noticed

how the corners have increased their contributions to the no-load flux linkage.

The no-load flux linkages for the four PM shapes investigated are computed and summarized in Table I. The no-load flux linkage calculated with FEA by using (5) is given in the second column, while the no-load flux linkage calculated by using (4) is given in the third column. The error $\Delta\lambda_{PM}$ shown in the fourth column, is the difference between columns 2 and 3 and is below 8% for all four PM configurations. This difference is due to the assumption of unity recoil permeability in the third column, as explained in [2].

From Table I, it can be concluded that the common practice of using square PMs with a width of 80% of the pole pitch does not lead to the highest ratio of λ_{PM}/V_{PM} . The configurations of Fig. 4 and Fig. 7 lead to higher ratios of λ_{PM}/V_{PM} . This result is specific to the pole geometry used in this example and should not be generalized to all pole pitches or machine types. However, it clearly shows the potential of the proposed method, which is applicable to any magnetic geometry with permanent magnets.

It must be stressed that a configuration with varying angles of B_r may be difficult to accomplish in practice. For example, the small corner PM pieces of Fig. 7 have a cross section of only 2 mm by 1.5 mm. It is probably not suitable to mount such small pieces in a production environment. The best choice is probably to magnetize the complete PM with a nonuniform field pattern similar to the field H_a created by the stator winding in the machine. As discussed by [6], PM materials such as ferrite, plastic-bonded Nd-Fe-B, Al-Ni-Co are isotropic and can be magnetized with various angles inside a same piece. However, materials with high-energy products such as sintered Nd-Fe-B and Sm-Co are usually anisotropic and, therefore, will exhibit one main direction of magnetization inside a given piece.

VI. DISCUSSION: DEMAGNETIZATION AND EFFICIENCY

This paper has investigated the use of alternate shapes and magnetization orientations for permanent magnets. The aim here is to obtain as high a no-load flux-linkage as possible. It must be pointed out that machine power is a combination of voltage and current. Increasing the no-load flux linkage will certainly affect the voltage in a positive way. However, nothing is said in the paper concerning the possible demagnetization of the permanent magnets. It was not the aim of this paper. But clearly, all different magnet shapes will have different values of flux density B_{PM} inside their volumes. This may result in some parts of a given magnet shapes being more sensitive to demagnetization. This could affect the nominal current that can possibly be fed to the machine. This topic is left for further investigations.

A note must also be made on the total machine efficiency. The method described in this paper aims at reducing the machine costs, by the optimization of the PM volume. However, efficiency is also an important factor which will be affected by the choice of the PM geometry. A given PM geometry will give a certain no-load flux linkage, which in turn will induce a no-load voltage. It may be the case that a high ratio of λ_{PM}/V_{PM} is obtained with a lower value of λ_{PM} . In such a case, the copper

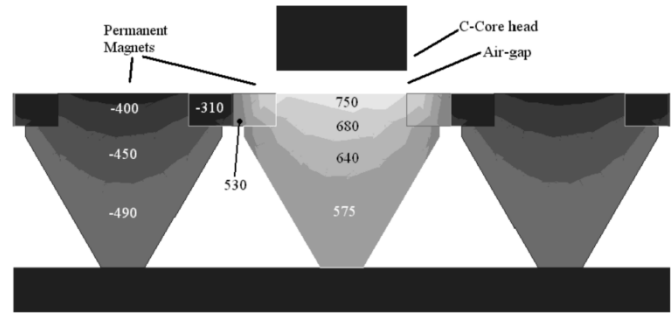


Fig. 8. Distribution of the product of $H_a \cdot B_r$, after insertion of small magnets in the corner of the main magnets.

losses in the stator will not be changed, while the total machine power will be reduced, thus resulting in lower efficiency. As it was the case for demagnetization, efficiency is not taken in consideration in the method presented here. However, both demagnetization and efficiency should be checked in the final machine design.

VII. CONCLUSION

A method proposed in [2] is applied to a machine with a small pole pitch (1 cm), i.e., a transverse-flux machine with single-sided surface-mounted PM. The method is used to increase the no-load flux linkage generated by the PM in the winding per volume of PM material. An enhancement of the method proposed in [2] is given in this paper, where the contribution of certain areas inside the PM volume to the no-load flux linkage is increased by varying their angle of magnetization. The result is an increase of 48% of the no-load flux linkage per volume of PM compared to the case of rectangular PM covering the total span of the pole pitch. An increase of 24% is also obtained compared to the common practice of using PM covering 80% of the pole pitch. According to this method, a PM should be magnetized by using a magnetic circuit similar to the magnetic circuit found in its natural location inside the machine. The magnetizing circuit would include the fringing stator-created magnetic field in the air gap instead of using magnet blocks premagnetized with a uniform and unidirectional direction of magnetization.

The no-load flux linkage calculated with (2) shows a maximum error of 8% compared to the conventional expression of no-load flux linkage given by (1). This error is attributed to the assumption in (2) of unity recoil permeability for the PM material. The deviation is small and the proposed method of computing no-load flux linkage appears as a valid tool for the optimization of PM shapes.

APPENDIX

The specifications and dimensions for the four pole geometries of Figs. 3, 4, 5, and 8 are as follows:

- PM remanent flux density $B_r = 1.23$ T;
- PM relative recoil demagnetization $\mu_{rec} = 1.09$;
- Distance between two C-cores = 20 mm;
- Width of stator C-core legs = 6 mm;
- Thickness of the air gap = 1 mm;
- Number of turns in the stator coil $n = 1$.

Dimensions Fig. 2:

- Width of PM = 10 mm;
- Distance between PM = 0 mm;
- Thickness of PM = 8 mm
- Total area of PM per magnet = 80 mm²;
- Total area of PM per C-core = 320 mm².

Dimensions Fig. 3:

- Width of PM = 8 mm;
- Distance between PM = 2 mm;
- Thickness of PM = 8 mm;
- Total area of PM per magnet = 64 mm²;
- Total area of PM per C-core = 256 mm².

Dimensions Fig. 4:

- Width of PM in the top part = 9 mm;
- Distance between PM in the top part = 1 mm;
- Width of PM in the bottom part = 2 mm;
- Distance between PM in the bottom part = 8 mm;
- Total thickness of PM = 8 mm;
- Thickness of the top (rectangular) part of the PM = 2 mm;
- Total area of PM per magnet = 51 mm²;
- Total area of PM per C-core = 204 mm².

Dimensions Fig. 7:

- Width of PM in the top part = 10 mm;
- Distance between PM in the top part = 0 mm;
- Width of PM in the bottom part = 2 mm;
- Distance between PM in the bottom part = 8 mm;
- Width of each PM element with 26° angle = 2 mm;
- Total thickness of PM = 8 mm;
- Thickness of the PM element with 26° angle = 1.5 mm;
- Total area of PM per magnet = 52.5 mm²;
- Total area of PM per C-core = 210 mm².

REFERENCES

- [1] A. Grauers, "Design of direct-driven permanent-magnet generators for wind turbines," Ph.D. dissertation, University of Goteborg, Sweden, 1996.
- [2] M. R. Dubois, H. Polinder, and J. A. Ferreira, "Contribution of permanent magnet volume elements to no-load voltage in machines," *IEEE Trans. Magn.*, vol. 39, pp. 1784–1792, May 2003.
- [3] M. R. Harris, G. H. Pajooman, and S. M. Abu Sharkh, "Performance and design optimization of electric motors with heteropolar surface magnets and homopolar windings," *Proc. Inst. Elect. Eng.—Electr. Power Appl.*, vol. 143, no. 6, pp. 429–436, Nov. 1996.

- [4] B. C. Mecrow, A. G. Jack, and C. P. Maddison, "Permanent magnet machines for high torque, low speed applications," in *Proc. Int. Conf. Elec. Mach.*, Vigo, Spain, 1996, pp. 461–466.
- [5] C. P. Maddison, B. C. Mecrow, and A. G. Jack, "Claw pole geometries for high performance transverse flux machines," in *Proc. Int. Conf. Elec. Mach.*, Turkey, 1998.
- [6] A. K. Adnanes, "High efficiency, high performance permanent magnet synchronous motor drives," Ph.D. dissertation, Univ. Trondheim, Norway, 1991.

Maxime R. Dubois (M'00) was born in Alma, QC, Canada, in 1968. He received the B.Eng. and M.Sc. degrees in electrical engineering from the Université Laval, Quebec, Canada, in 1991 and 1993, respectively. He is working toward the Ph.D. degree at the Laboratory of Electrical Power Processing, Delft University of Technology, Delft, The Netherlands.

Between 1993 and 1999, he worked as a design engineer for private companies in Canada in the area of power electronics. Since 1999, he has been with the Laboratory of Electrical Power Processing, Delft University of Technology. His main interests are machines and power electronics applied to the generation of energy from renewable sources.

Henk Polinder (M'97) was born in Nunspeet, The Netherlands, in 1968. He received the M.Sc. degree in 1992 and the Ph.D. degree in 1998, both in electrical engineering, from Delft University of Technology, Delft, The Netherlands.

Currently, he is an Assistant Professor at the Electrical Power Processing Laboratory, Delft University of Technology, where he teaches courses on electrical machines and drives. His research interests are in the field of electromechanical power conversion. He currently works on direct drive generators for wind turbines, linear direct drive generators for wave energy, and actuators for high-precision motion control.

Jan A. Ferreira (M'88–SM'01) was born in Pretoria, South Africa. He received the B.Sc.Eng. (*cum laude*), M.Sc.Eng. (*cum laude*), and Ph.D. degrees in electrical engineering from the Rand Afrikaans University, Johannesburg, South Africa, in 1980, 1982, and 1988, respectively.

In 1981, he was with the Institute of Power Electronics and Electric Drives, Technical University of Aachen, Aachen, Germany, and worked in industry at ESD(Pty) Ltd from 1982 to 1985. From 1986 to 1997, he was on the Faculty of Engineering at Rand Afrikaans University, where he held the Carl and Emily Fuchs Chair of Power Electronics. Since 1998, he has been a Professor at the ITS Faculty of the Delft University of Technology, Delft, The Netherlands.

Prof. Ferreira is the Transactions Review Chairman of the IEEE IAS Power Electronic Devices and Components Committee, Vice-Chairman of the IEEE Joint IAS/PELS Benelux chapter, and Chairman of the CIGRE SC14 national committee of the Netherlands. He is also a member of the IEEE PESC Adcom and a member of the executive committee of the EPE Society.